Fuel 207 (2017) 262–267

Contents lists available at ScienceDirect

Fuel

journal homepage: www.elsevier.com/locate/fuel

Three-dimensional optical tomography of bitumen and clay association in oil sands tailings

Sarang Pendharker [a,1], Swapnali Shende [b,1], Zubin Jacob [a,c], Neda Nazemifard [b,*]

[a] Department of Electrical and Computer Engineering, University of Alberta, Edmonton, Alberta T6G 1H9, Canada
[b] Department of Chemical and Materials Engineering, University of Alberta, Edmonton, Alberta T6G 1H9, Canada
[c] Department of Electrical Engineering, Purdue University, West Lafayette, IN 47907, United States

ARTICLE INFO

Article history:
Received 12 April 2017
Received in revised form 7 June 2017
Accepted 21 June 2017
Available online 28 June 2017

Keywords:
Oilsands
Bitumen
Mature Fine Tailings (MFT)
Total Internal Reflection Fluorescence (TIRF) microscopy
Clay
Tomography

ABSTRACT

Alberta has one of the largest oil reserves in the world. Large-scale commercial oil production from oil sands in Alberta for the past 40 years has led to accumulation of tailings water in tailings ponds covering areas ranging over 150 km^2. Less than 1% of this area has been certified as reclaimed leading to both economic and environmental consequences. Research is underway to reduce tailings ponds reclamation time from decades to weeks by developing new polymer flocculants, better tailings treatment methods and recovering bitumen from tailings. Information about impact of residual bitumen on the shear strength, trafficability, densification, hydraulic conductivity, consolidation, post-reclamation settlement for oil sands tailings is insufficient. Outstanding challenges exist in understanding bitumen and clay interaction in tailings to help with the development of techniques which accelerate clay sedimentation and enhance bitumen recovery. To shed light on the bitumen-clay interactions, here we develop advanced three-dimensional optical tomography approaches approaching sub-micron resolution. In this paper, we report, the first ever Total Internal Reflection Fluorescence (TIRF) microscope tomography for Mature Fine Tailings (MFT) samples to reveal bitumen distribution on clay in MFT. We employ a unique evanescent wave illumination approach as opposed to conventional fluorescence microscopy with enhanced axial resolution and high signal-to-noise ratio. The resolution of TIRF is further improved by using an Axial Super-Resolution Evanescent-wave Tomography (AxSET) technique. The information obtained from this study not only gives evidence of the presence of hydrophilic and oleophilic clays but with aid of 3D reconstruction using advance image processing also validates that bitumen is partially coating some of clay surfaces, thus verifying the presence of biwettable clays in oil sands MFT. The advances from our imaging work can aid the development of bitumen recovery techniques for environmental and economic impact.

1. Introduction

Oil sands deposits covering over 14000 km^2 and estimated recoverable oil reserves over 300 billion barrels makes this non-conventional oil a major economic driver of Alberta and Canada at large. Oil sands composition can be described as 55–80 wt% sands, 4–18 wt% bitumen, 5–34 wt% fine solids (less than 45 μm), and 2–15 wt% water [1]. Processability of ore can be determined by ease of bitumen detachment from clays and ease of bitumen attachment to the air bubbles [2]. Extraction techniques namely Clark Hot Water Extraction (CHWE) Process and Low Energy Extraction (LEE) Process [3] which are used commercially for oil sands extraction, require hydrophobic nature of the minerals that are separated from the bitumen by an aqueous layer [4]. The presence of biwettable and hydrophobic minerals in oil sands negatively impacts bitumen recovery and froth quality [5].

Efficient recovery of bitumen from oil sands and reduction of its loss to tailings is important economically as well as environmentally. Absence of bitumen in tailings can also reduce the severity of failure of containment events due to relatively reduced toxicity of the tailings. Presence of bitumen in tailings reduces its hydraulic conductivity and consolidation interactions [6]. Bitumen in tailings is suspected to hinder its settling by associating with clays [7]. These bitumen-clay interactions take place at a nanoscale [8].

Methods such as Transmission Electron Microscopy (TEM) [9] and X-ray Diffraction (XRD) [10,11] have been used to characterize various clays in oil sands and oil sands tailings. Researchers have

* Corresponding author.
E-mail addresses: sarang.pendharker@ualberta.ca (S. Pendharker), sshende@ualberta.ca (S. Shende), zjacob@purdue.edu (Z. Jacob), nn1@ualberta.ca (N. Nazemifard).
[1] The first two authors contributed equally to this work.

http://dx.doi.org/10.1016/j.fuel.2017.06.107
0016-2361/

also used techniques such as Scanning Electron Microscope (SEM) [12] and Atomic Force Microscope (AFM) [13] to study bitumen-clay interactions. But extensive sample preparation and highly altered temperature and pressure conditions are suspected to affect sample chemistry and introduce artifacts in the acquired images [12]. These techniques are also not successful in detecting organic materials. Hence bitumen locations and interaction needs to be inferred in these studies [14]. Techniques such as deak stark [12] and CHNS analysis [15] are used to detect the bitumen content of the oil sands and oil sands tailings but this method does not provide information about free bitumen versus bitumen attached to clay. Studies to detect the exact spacial location of bitumen on clay surface are not yet available. This knowledge will help to obtain clear picture about bitumen-clay interaction and hence help propose solutions to enhance bitumen recovery from oil sands.

Since bitumen has been proved to show natural fluorescence [7] similar to asphaltenes [16] over a relatively broad emission spectrum, therefore successful detection of bitumen in the MFT samples can be achieved with novel techniques involving fluorescence. Techniques such spectrofluorometery have been used in our study in past, to confirm the favorable excitation and emission wavelengths for fluorescence microscopy of bitumen [17]. Confocal fluorescence microscope was also used in this study to ensure that only bitumen will show fluorescence while water and clay will not [17]. These techniques have been mainly utilized in the cell biology field but are recently gaining importance in material sciences as well.

In this paper we present the first direct three dimensional visualization of bitumen covering the clay particles in oil-sands tailings sample. We show the bitumen coverage of clay particles at multiple scales, ranging from 4–5 μm bitumen clay agglomerates to sub-micron single particle coverages. We employ Axial Super-Resolution Evanescent-wave Tomography (AxSET) technique, which was recently developed in our group [18], to get 3D reconstruction of sub-micron scale bitumen clay association with axial super-resolution.These 3D maps of bitumen-clay aggregates have assisted in obtaining first ever images of the non-uniform bitumen coatings in tailings samples. These 3D reconstruction provide valuable insight into bitumen surface associations which will ultimately aid in improving the techniques for tailings treatment. This method can also be successfully employed in oil sands and bitumen froth.

2. Experimental

Mature Fine Tailings (MFT) sample A, B and C were provided by Institute of Oil Sands Innovation (IOSI), University of Alberta. Samples A and B contain approximately 31.4 wt% solids, 3.9 wt% bitumen and 64.7 wt% water. Sample C contained approximately 67.6 wt% water, 28.8 wt% solids, and 3.6 wt% bitumen. The solids, bitumen and water content in these samples was analyzed using dean stark method.

MFT samples were observed without drying to ensure that they are observed in their original state. To enable this, well-type coverslips were made by gluing the coverslip on to a glass slide that has a 10 mm diameter circular aperture drilled in its center. MFT samples were placed in these wells and then sealed on the top with another glass cover to prevent drying or contamination as seen in Fig. 1(b).

2.1. Evanescent wave tomography

Fig. 1(a) depicts the schematic of a Total Internal Reflection Fluorescence (TIRF) microscope used in tomographic imaging of

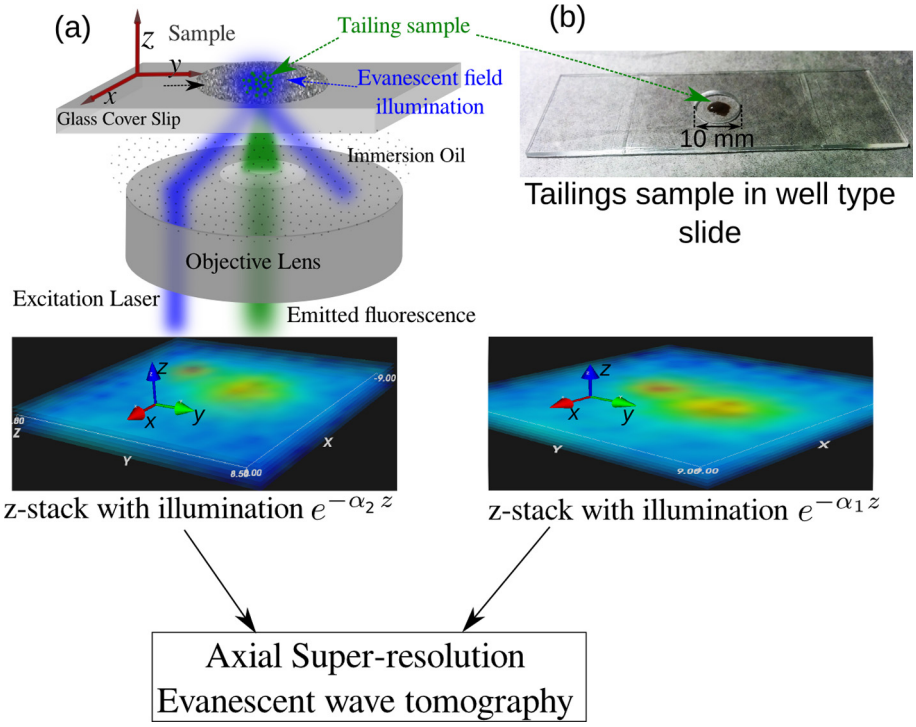

Fig. 1. (a) Schematic of TIRF microscope, in which the incident angle of the excitation laser can be controlled. When the incident angle is greater than the critical angle at the cover-slip/sample interface, the sample is illuminated by an evanescent wave. By controlling the incident angle of the excitation laser (blue) the penetration depth of the evanescent wave can be controlled. (b) shows the tailings sample in a well type cover-slip. Two 3-dimensional images are acquired by optical sectioning of the sample with different penetration depth of the evanescent wave excitation. Axial super-resolution is achieved by extracting the super-resolution features from incremental illumination of the sample from the two 3D images in the Fourier domain [18]. (For interpretation of the references to colour in this figure legend, the reader is referred to the web version of this article.)

bitumen present in the oil-sands sample. In TIRF microscopy, a fluorescent sample is illuminated with evanescent wave generated by total internal reflection at the interface of coverslip and the sample [19,20]. For total internal reflection to occur, the refractive index of the sample should be less than that of glass coverslip (1.55). Since the MFT sample contains water as the continuous phase, its the refractive index is close to that of water (1.33), with small local variations across the sample. The condition for total internal reflection is therefore satisfied by the MFT samples.

By controlling the incident angle of the excitation laser, the penetration depth of the evanescent wave can be controlled [19]. The illumination profile of the evanescent wave is given by $e^{-\alpha z}$, where α is the attenuation coefficient of the wave, and the illumination depth is given by $dz = 1/\alpha = \lambda/(2\pi\sqrt{n_c^2 \sin(\theta) - n_s^2})$, where λ is the wavelength of excitation laser, θ is the incident angle and n_c and n_s are the refractive index of the coverslip and the sample, respectively. For 488 nm excitation laser, and a refractive index contrast of 1.33 (water) and 1.55 (cover-slip), the penetration depth can be controlled between $\sim$ 100 nm (for $\sin\theta \to 1$) and bulk illumination (θ is close to critical angle). Generally, TIRF microscope is used to capture near-surface 2D images of a sample. However, here we extend the capability of TIRF and use it to acquire 3D tomographic images with high signal-to-noise ratio, by acquiring multiple z-stack images near the critical angle as shown in Fig. 1. The axial resolution of the acquired 3D image is limited by the axial resolution of the objective lens of the microscope, which is 2–3 times worse than the focal plane resolution [21]. To get resolution higher than the axial resolution of the microscope we use a recently reported method of Axial Super-resolution Evanescent Wave Tomography (AxSET) [18], where we capture two 3D images at varying penetration depths, and extract the super-resolution features from the incremental penetration of the excitation laser, in the Fourier domain. This method is described in detail in [18].

A Nikon eclipse Ti TIRF was used in our microscopy. It was facilitated with 488 nm, 543 nm and 633 nm lasers manufactured by Melles Griot. 488 nm laser was used for excitation and fluorescence in the range 500–550 nm was collected for imaging. Highly sensitive QuantEM 512sc CCD camera using 512x512 pixels was employed for capturing TIRF images. For the imaging, a 100× objective was used.

3. Results and discussion

Using spectrofluorometer it was confirmed that 488 nm laser would be appropriate for the fluorescence microscopy of MFT sample [17]. Using confocal fluorescence microscope it was established that in MFT sample, clay and water do not show fluorescence. The TIRF images of MFT sample showed the presence of fluorescing bitumen in pool of non-fluorescing water and clay. To understand the bitumen distribution in MFT sample, the constraint was the bright field images which did not clearly show the boundaries of clay, and 2D images were inadequate to capture the surface coverage and morphology of the bitumen on clay particles.

Since all previous MFT images [17] showed strongly fluorescing particles, it was realized that reducing the laser intensity could reduce their glare and aid with imaging minute features within the fluorescing particles. This also reduced photo-bleaching of the sample, resulting in better subsequent 3D imaging. The intensity

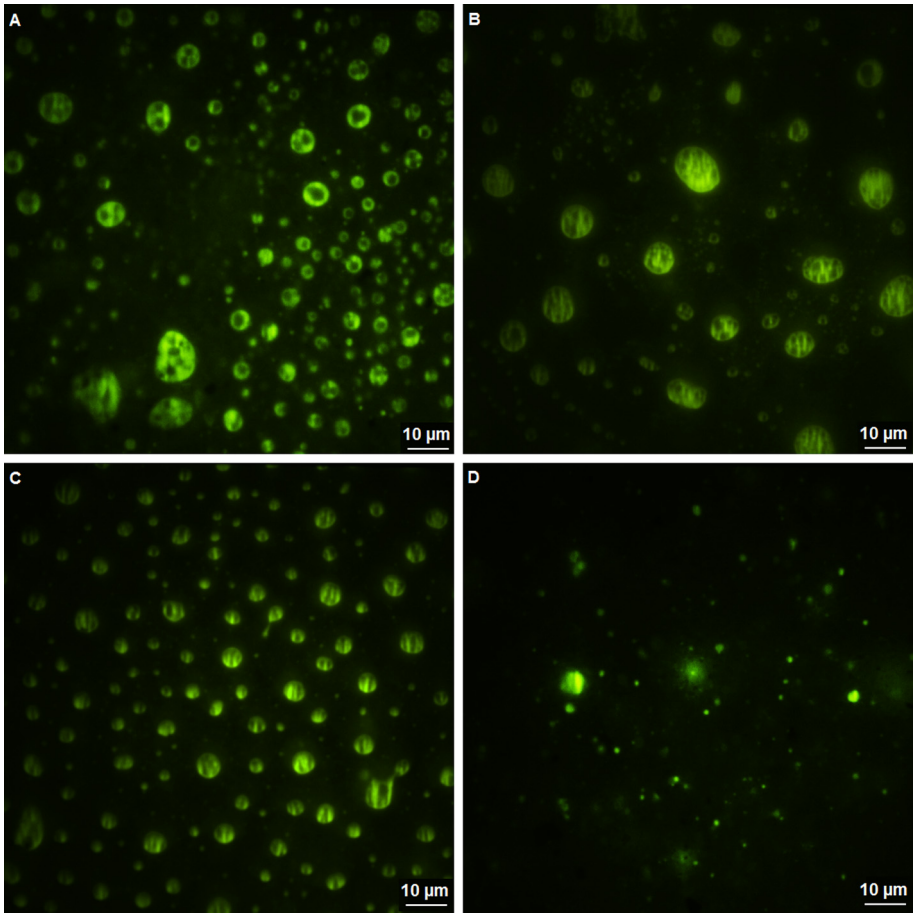

Fig. 2. Images A and B are the TIRF image of sample B. Image C is the TIRF image of sample A and image D is TIRF image of sample C. These images were taken with reduced laser intensity. They show the features within the fluorescing bitumen coating. Sample C show smaller fluorescing aggregates compared the sample A and B.

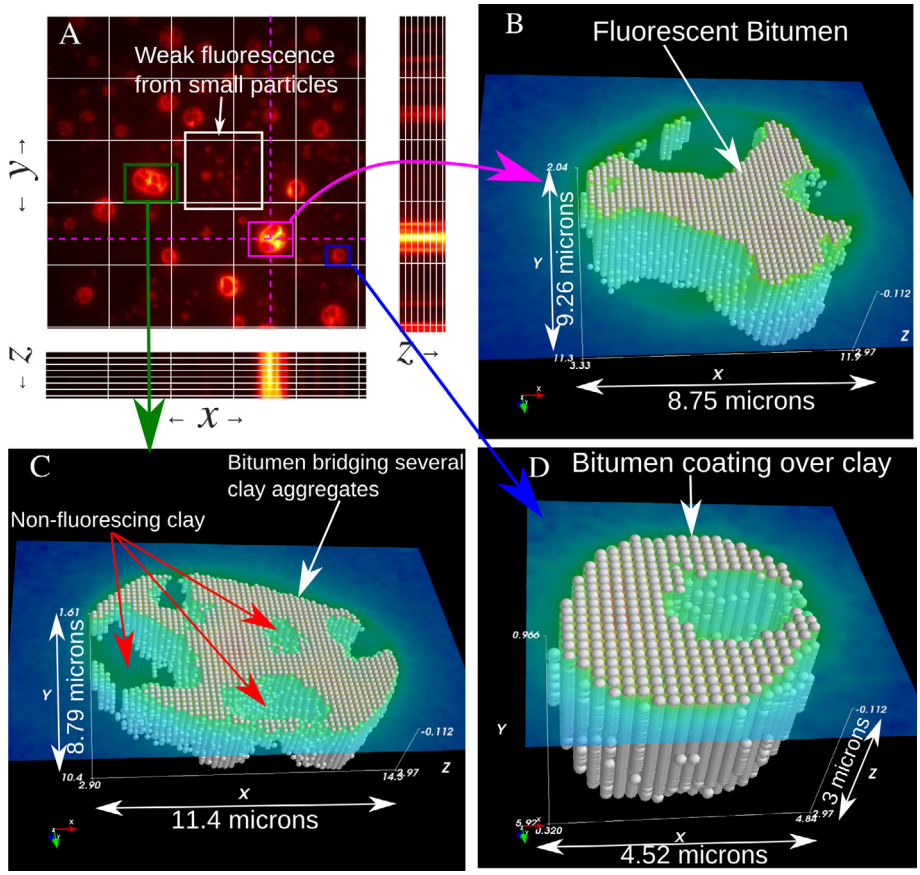

Fig. 3. Image A is the optical section of the TIRF z-stack images for sample B. Image B, C and D show the 3D reconstruction of an aggregate in the image A. It is apparent from these images that bitumen coating on these clay aggregates is non-uniform. There are regions on some of the clay surfaces where bitumen coating is absent.

of laser on the samples was reduced by introducing an optical attenuator in the path of excitation laser. The images obtained after laser intensity reduction are shown in Fig. 2. To ensure repeatability of the results, three different MFT samples, sample A, B and C were imaged.

Fig. 2, clearly show the presence of non-uniform bitumen coating. The presence of non-uniform bitumen coating, can be clearly observed in the image A of Fig. 3, which shows the fluorescing aggregates along with the cross-sectional view, visualized using 'hot' colormap which accentuates the features. The bright spots in the image represent high fluorescence from the bitumen. Image B, C and D of Fig. 3 and image C of Fig. 4, show three-dimensional tomographic reconstruction from the 3D image. The Three-dimensional images of the samples were acquired by z-stacking multiple focal-plane optical sections, from which the 3D image reconstructions of individual particles were created by thresholding and segmenting the image over selected region-of-interest. Fig. 4(B) shows the focal-plane and axial-plane cross-sections of the a bitumen coverage of clay particle, and panel C shows the corresponding 3D reconstruction. It can be clearly observed in these images that the bitumen coats and covers inorganic clay aggregates and forms bigger cluster by bridging several clay aggregates (see panel B and C of Fig. 3). It is also evident that the bitumen coverage of clay is not uniform and coats the inorganic clay partially. In both figures, Fig. 3 and Fig. 4, along with bright and large (5–10 μm) bitumen-clay clusters, we can also observe weak fluorescence from small particles, as indicated in the white box in the figures. These weak fluorescence is due to thin bitumen coverage in smaller particles.

Since the acquired 3D images are diffraction limited, their resolution in axial direction is particularly inferior ($>$ 450 nm), which hinders the estimation of thickness of bitumen coverage on small clay particles. Therefore, we apply the AxSET technique developed by our group [18], and explained in Section 2.1, to reconstruct bitumen coating over a thickness of $\sim$ 1 μm. Fig. 5 shows the AxSET reconstruction of bitumen coverage of clay particles at sub-micron scale. Fig. 5(a) shows the a focal plane image of the tailing sample and three regions of interest marked by (b), (c) and (d), over which AxSET is performed. The reconstructed AxSET images showing sub-micron bitumen coatings are shown in the corresponding panels (b), (c) and (d). In all the three AxSET reconstructions of bitumen, it can be seen that fluorescing material envelops non-fluorescing region, indicating the bitumen coverage of inorganic clay, even in the weakly fluorescing particles. The weak fluorescence is due to the thin sub-micron coating of bitumen around inorganic clay. The bitumen coating in some regions is as thin as 250–300 nm. These sub-micron bitumen coverages are present in tailings alongside the large bitumen-clay aggregates shown in Figs. 3 and 4, and emit extremely faint fluorescence compared to the thick bitumen coatings. Fig. 5(d) shows the presence of larger blob of bitumen alongside thin and faint fluorescence from thin bitumen sticking around inorganic clay.

These images emphasize and prove the heterogeneity of surface properties of clay aggregates in oil sands MFT [22,23]. In these images, the presence of clay surfaces with and without bitumen coating can be noted. These images are an evidence of presence of biwettable clays in oil sands.

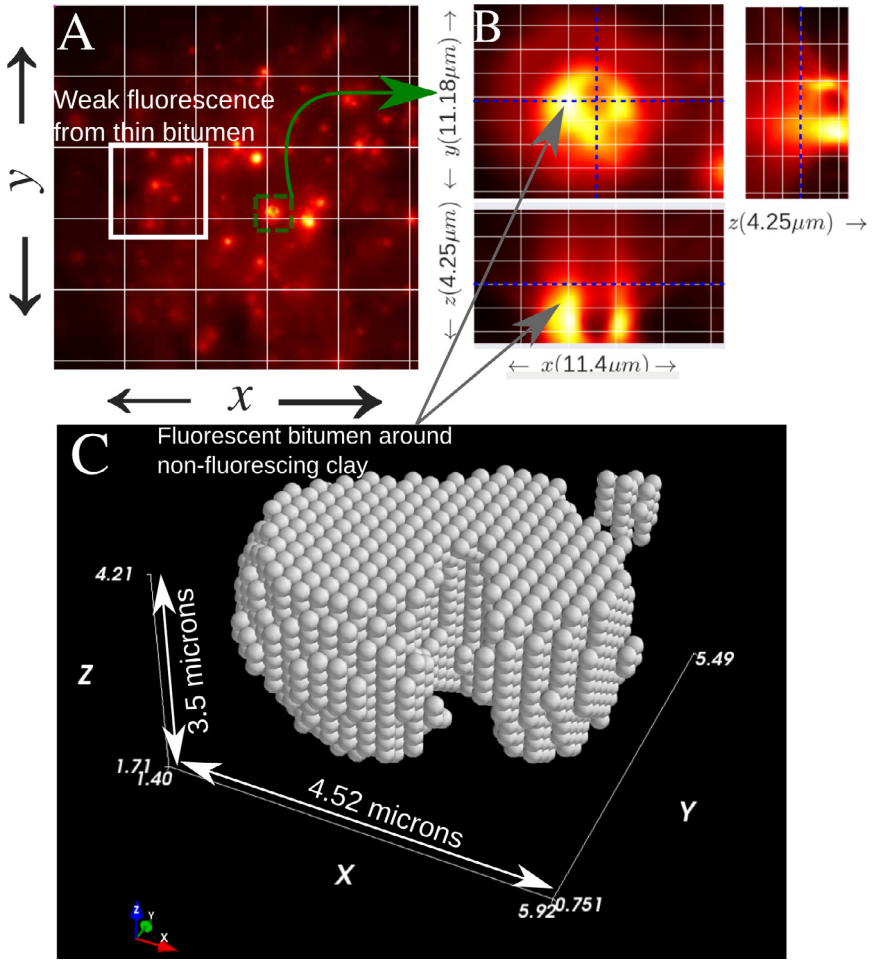

Fig. 4. Image A is the optical section of the TIRF z-stack images for sample B. Image B depicts region of interest with focus on a single aggregate. Image C is the 3D reconstruction of the single aggregate in image B. The uneven bitumen coating can be clearly seen in these images.

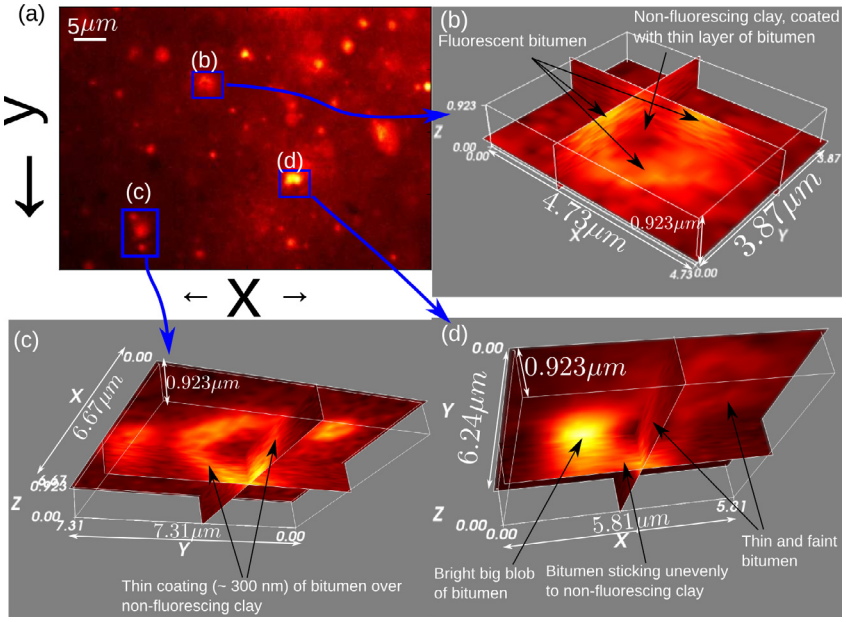

Fig. 5. Sub-micron 3D reconstruction of bitumen coating in Sample B with axial super-resolution, generated by AxSET. (a) shows the $x - y$ plane (focal plane) image of the tailings sample. z-stack of multiple focal plane images, acquired at two illumination angles (with different penetration depths) are processed by AxSET to get 3D reconstruction of bitumen over sample thickness of ~ 1 μm. The 3D reconstruction three regions, marked by blue rectangles in (a) are shown in panel (b), (c) and (d). The 3D reconstructions show sub-micron non-uniform coating of bitumen on clay particles, which emit weak fluorescence in the tailings sample. (For interpretation of the references to colour in this figure legend, the reader is referred to the web version of this article.)

4. Conclusion

In order to lower the economic and environmental impact of tailings, research is being performed to reduce the land reclamation time to the order of few weeks, to recycle the water at process temperature and minimize the amount of additional fresh water requirement. Multiple studies have advised that bitumen in tailings has detrimental effect on the aggregation and consolidation of clays in tailings. High resolution electron microscopes have been used to understand the clay and bitumen interaction. Since these techniques are inorganic material specific, they can only hypothesize the bitumen location. The first ever TIRF tomography performed in this study, has paved way towards clear visualization of bitumen location and interaction in MFT.

The results from this study show detailed features of and within the fluorescing bitumen aggregates which confirm the presence of hydrophobic and biwettable clay aggregate. The occurrence of clay surfaces which are fully as well as partially coated with bitumen are clearly obtained with this technique. With the aid of 3D reconstruction of bitumen clay aggregates in MFT, the existence of non-uniform bitumen coating on the clay surface can be observed. The well type slides ensure that these samples are imaged in their original state.AxSET technique used here, provides higher axial resolution which further improves the knowledge regarding surfaces and boundaries of these aggregates.

Currently, correlative imaging of MFT samples with TIRF and other high resolution techniques such as He-ion microscopy, which requires minimal sample alteration and gives sub-nanometer resolution is being performed in our group to reveal whether the basal plane or edge of clay surface is interacting with bitumen. This will give better understanding about the bitumen-clay interactions in MFT and help in development of improved tailings treatments and/ or polymer flocculants. Exploring this technique in Froth studies can also help obtain information regarding the bitumen-air and bitumen-clay attachment for a industrial sample which will assist in improving efficiency of the process.

Acknowledgements

The authors acknowledge the financial support of Institute for Oil Sands Innovation (IOSI), Canada. We are also grateful to Dr. Xiaoli Tan and Gareth Lambkin for all their help and technical support. The authors would like to acknowledge the access to OSCIEF equipment at NINT and Biological Services equipment in Chemistry department in University of Alberta. The authors would also like to thank Dr. Gan Weibing for his insightful comments throughout this work.

References

[1] Bichard JA. Oil Sands Composition and Behaviour Research: The Research Papers of John A. Bichard, 1957–1965, Alberta Oil Sands Technology and Research Authority, 1987.
[2] Liu J, Xu Z, Masliyah J. Processability of oil sand ores in alberta. Energy Fuels 2005;19(5):2056–63.
[3] F.T. Fundamentals, Advances in oil sands tailings research, Alberta, Canada: Alberta Dept. of Energy, Oil Sands and Research Division.
[4] Takamura K. Microscopic structure of athabasca oil sand. Can J Chem Eng 1982;60(4):538–45.
[5] Dang-Vu T, Jha R, Wu S-Y, Tannant DD, Masliyah J, Xu Z. Effect of solid wettability on processability of oil sands ores. Energy Fuels 2009;23 (5):2628–36.
[6] Chow R, McKenna G, Win S, Journault J. A. Innovates-Energy, E. Solutions, C.T.E. P. Area, Recovery of Bitumen from Oil Sands Tailings Streams and Deposits: Potential Opportunities and Benefits; 2014. URL https://books.google.ca/books?id=3iPNrQEACAAJ.
[7] Mikula R, Munoz V. Characterization of emulsions and suspensions in the petroleum industry using cryo-sem and clsm. Colloids Surf A: Physicochemical Eng Aspects 2000;174(1):23–36.
[8] Johnston CT. Probing the nanoscale architecture of clay minerals. Clay Miner 2010;45(3):245–79.
[9] Ahn J, Peacor D. Transmission and analytical electron microscopy of the smectite-to-illite transition. Clays Clay Miner 1986;34(2):165–79.
[10] Liu H, Tan S, Yu T, Liu Y. Sulfate reducing bacterial community and in situ activity in mature fine tailings analyzed by real time qpcr and microsensor. J Environ Sci 2016;44:141–7.
[11] Omotoso OE, Munoz VA, Mikula RJ. Mechanisms of crude oil–mineral interactions. Spill Sci Technol Bull 2002;8(1):45–54.
[12] Hooshiar A, Uhlik P, Liu Q, Etsell TH, Ivey DG. Clay minerals in nonaqueous extraction of bitumen from alberta oil sands: Part 1. nonaqueous extraction procedure. Fuel Process Technol 2012;94(1):80–5.
[13] Liu J, Xu Z, Masliyah J. Role of fine clays in bitumen extraction from oil sands. AIChE J 2004;50(8):1917–27.
[14] Li H, Long J, Xu Z, Masliyah JH. Novel polymer aids for low-grade oil sand ore processing. Can J Chem Eng 2008;86(2):168–76.
[15] Zhao S, Kotlyar LS, Sparks BD, Woods JR, Gao J, Chung KH. Solids contents, properties and molecular structures of asphaltenes from different oilsands. Fuel 2001;80(13):1907–14.
[16] Zhang HT, Li R, Yang Z, Yin C-X, Gray MR, Bohne C. Evaluating steady-state and time-resolved fluorescence as a tool to study the behavior of asphaltene in toluene. Photochem Photobiolog Sci 2014;13(6):917–28.
[17] Shende SS, Pendharker S, Jacob Z, Nazemifard N. Total internal reflection fluorescence microscopy to investigate the distribution of residual bitumen in oil sands tailings. Energy Fuels 2016.
[18] Pendharker S, Shende S, Newman W, Ogg S, Nazemifard N, Jacob Z. Axial super-resolution evanescent wave tomography. Opt Lett 2016;41 (23):5499–502.
[19] Axelrod D. Total internal reflection fluorescence microscopy. Methods Cell Biol 2008;89:169–221.
[20] Shen H, Huang E, Das T, Xu H, Ellisman M, Liu Z. Tirf microscopy with ultra-short penetration depth. Opt Express 2014;22(9):10728–34.
[21] Hell SW, Wichmann J. Breaking the diffraction resolution limit by stimulated emission: stimulated-emission-depletion fluorescence microscopy. Opt Lett 1994;19(11):780–2.
[22] Tombácz E, Szekeres M. Surface charge heterogeneity of kaolinite in aqueous suspension in comparison with montmorillonite. Appl Clay Sci 2006;34 (1):105–24.
[23] Liu J, Gaikwad R, Hande A, Das S, Thundat T. Mapping and quantifying surface charges on clay nanoparticles. Langmuir 2015;31(38):10469–76.